© 2013 by The American Society for Biochemistry and Molecular Biology, Inc.
This paper is available on line at http://www.mcponline.org

Quantitative Measurement of Phosphoproteome Response to Osmotic Stress in *Arabidopsis* Based on Library-Assisted eXtracted Ion Chromatogram (LAXIC)*[S]

Liang Xue‡, Pengcheng Wang§, Lianshui Wang¶, Emily Renzi‖, Predrag Radivojac¶, Haixu Tang¶, Randy Arnold‖, Jian-Kang Zhu§‖‖, and W. Andy Tao‡‡‡**

Global phosphorylation changes in plants in response to environmental stress have been relatively poorly characterized to date. Here we introduce a novel mass spectrometry-based label-free quantitation method that facilitates systematic profiling plant phosphoproteome changes with high efficiency and accuracy. This method employs synthetic peptide libraries tailored specifically as internal standards for complex phosphopeptide samples and accordingly, a local normalization algorithm, LAXIC, which calculates phosphopeptide abundance normalized locally with co-eluting library peptides. Normalization was achieved in a small time frame centered to each phosphopeptide to compensate for the diverse ion suppression effect across retention time. The label-free LAXIC method was further treated with a linear regression function to accurately measure phosphoproteome responses to osmotic stress in *Arabidopsis*. Among 2027 unique phosphopeptides identified and 1850 quantified phosphopeptides in *Arabidopsis* samples, 468 regulated phosphopeptides representing 497 phosphosites have shown significant changes. Several known and novel components in the abiotic stress pathway were identified, illustrating the capability of this method to identify critical signaling events among dynamic and complex phosphorylation. Further assessment of those regulated proteins may help shed light on phosphorylation response to osmotic stress in plants. ***Molecular & Cellular Proteomics 12: 10.1074/mcp.O113.027284, 2354–2369, 2013.***

Phosphorylation plays a pivotal role in the regulation of a majority of cellular processes via signaling transduction pathways. During the last decade, quantitative phosphoproteomics has become a powerful and versatile platform to profile signaling pathways at a system-wide scale. Multiple signaling networks in different organisms have been characterized through global phosphorylation profiling (1–3), which has evolved over the years with highly optimized procedures for sample preparation and phosphopeptide enrichment, high resolution mass spectrometry, and data analysis algorithms to identify and quantify thousands of phosphorylation events (4–8).

Quantitative phosphoproteomics can be achieved mainly by two major techniques, stable isotope labeling and label-free quantitation. Isotope labeling prior to liquid chromatography-mass spectrometry (LC-MS)[1] has been widely used, including metabolic labeling such as stable isotope labeling by amino acids in cell culture (SILAC), chemical labeling such as multiplexed isobaric tags for relative and absolute quantification (iTRAQ) and isotope-coded affinity tags (ICAT) (9–12). On the other hand, label-free quantitation has gained momentum in recent years (13–15), as no additional chemistry or sample preparation steps are required. Compared with stable isotope labeling, label-free quantitation has higher compatibility with the source of the samples, the number of samples for comparison, and the instrument choice.

Many label-free approaches, in particular to phosphoproteomics, are based on ion intensity (16, 17), but they are relatively error-prone because of run-to-run variations in LC/MS performance (18). In theory, such systematic errors can be corrected by spiking an internal standard into every sample to be compared. Several methods based on internal standard spiking have been reported so far. Absolute quantification peptide technology (AQUA) (19), for example, uses synthetic peptides with isotope labeling for absolute quanti-

From the ‡Departments of Biochemistry, Purdue University, West Lafayette, IN 47907; §Horticulture and Landscape Architecture, Purdue University, West Lafayette, IN 47907; ¶School of Informatics and Computing, Indiana University, Bloomington, IN 47405; ‖Department of Chemistry, Indiana University, Bloomington, IN 47405;‖‖Shanghai Center for Plant Stress Biology, Shanghai Institutes for Biological Sciences, Chinese Academy of Sciences, Shanghai 200032, China

Received January 5 2013, and in revised form, April 18, 2013
Published, MCP Papers in Press, May 8, 2013, DOI 10.1074/mcp.O113.027284

[1] The abbreviations used are: LC-MS, liquid chromatography-MS; ABA, abscisic acid; CV, coefficient of variation; FDR, false discovery rate; GO, gene ontology; LAXIC, Library Assisted eXtracted Ion Chromatogram; PBS, phosphate buffered saline; PolyMAC, polymer-based metal-ion affinity capture; SnRK, SNF-related serine/threonine-protein kinase; XIC, exacted ion chromatograms.

tation. For a global quantitative proteomics study, it is unrealistic to spike-in all reference peptides. Another labeling reference method, spike-in SILAC appears to be a promising technique to quantify the proteome *in vivo* with multiplex capability and it can be extended to clinical samples (20). One solution to large-scale quantitation without any isotope labeling is pseudo internal standard approach (21), which selects endogenous house-keeping proteins as the internal standard so that no spike-in reagent is required. However, finding a good pseudo internal standard remains a challenge for phosphoproteome samples. Spike-in experiments are an alternative way to improve normalization profile. Some internal standard peptides such as MassPREP™ (Waters) were already widely used. Other groups spiked an identical amount of standard protein into samples prior to protein digestion (22–24). There are two major normalization procedures. In one approach, sample peptides were normalized to the total peak intensity of spike-in peptides (25). Alternatively, the digested peptides were compared at first and the normalization factor was determined in different ways such as the median (26) or average of ratios (27). However, spiking an identical amount of standard proteins into phosphoproteomic samples before protein digestion may not be compatible with phosphoproteomic analyses which typically require a phosphopeptide enrichment step. Spectral counting has been extensively applied in large sets of proteomic samples because of its simplicity but the method is often not reliable for the quantitation of phosphoproteins, which are typically identified by single phosphopeptides with few spectra (28–30). Many software packages have been implemented to support the wide variety of those quantitation techniques, including commercial platforms such as Progenesis LC-MS™, Mascot Distiller™, PEAKS Q™, etc., as well as open-source software packages including MaxQuant (31), PEPPeR (32), Skyline (33), etc.

In this study, we have devised a novel label-free quantitation strategy termed Library Assisted eXtracted Ion Chromatogram (LAXIC) for plant phosphoproteomic analyses with high accuracy and consistency (Fig. 1). The approach employs synthetic peptide libraries as the internal standard. These peptides were prepared to have proper properties for quality control assessments and mass spectrometric measurements. In particular, peptides were designed to elute sequentially over an entire LC gradient and to have suitable ionization efficiency and *m/z* values within the normally scanned mass range. Local normalization of peak intensity is performed using Loess Procedure, a data treatment adopted from cDNA microarray data analysis (34). To monitor the diverse ion suppression effect across retention time, the local normalization factors (LNFs) are determined by internal standard pairs in individual time windows. Finally, samples will be quantified with LNFs in order to correct variance of LC-MS conditions. This quantification occurs in a small time frame centered to each target peptide.

Water deficit and salinity causes osmotic stress, which is a major environmental factor limiting plant agricultural productivity. Osmotic stress rapidly changes the metabolism, gene expression and development of plant cells by activating several signaling pathways. Several protein kinases have been characterized as key components in osmotic stress signaling. *Arabidopsis* histidine kinase AHK1 can complement the histidine kinase mutant yeast, which can act as the osmosensor in yeast (35). Overexpression of AHK1 gene increases the drought tolerance of transgenic plants in *Arabidopsis* (36). Similar to yeast, the MAPK kinase cascade is also involved in osmotic stress response in plants. It is reported that AtMPK3, AtMPK6, and tobacco SIPK can be activated by NaCl or mannitol, and play positive roles in osmotic signaling (37, 38). MKK7 and MKKK20 may act as the up-stream kinase in the kinase cascade (39). Involvement of some calcium-dependent protein kinases, such as AtCPK21, AtCPK6, and OsCPK7 (CDPK) in osmotic stress signaling has also been reported (40–42). Another kinase family, SNF1-related protein kinase (SnRK) 2, also participates in osmotic stress response. In *Arabidopsis*, there are ten members in the SnRK2 family. Five from the ten SnRK2s, SnRK2, 3, 6, 7, and 8, can be activated by abscisic acid (ABA) and play central roles in ABA-receptor coupled signaling (43, 44). Furthermore, all SnRK2s except SnRK2.9 can be activated by NaCl or mannitol treatment (43). The decuple mutant of SnRK2 showed a strong osmotic hypersensitive phenotype (45). It is proposed that protein kinases including MAPK and SnRK2s have a critical function in osmotic stress (46), but the detailed mechanism and downstream substrates or target signal components are not yet clarified. We applied, therefore, the LAXIC approach with a self-validating method (47) to profile the osmotic stress-dependent phosphoproteome in *Arabidopsis* by quantifying phosphorylation events before and after mannitol treatment. Among a total of over 2000 phosphopeptides, more than 400 of them are dependent on osmotic stress. Those phosphoproteins are present on enzymes participating in signaling networks that are involved in many processes such as signal transduction, cytoskeleton development, and apoptosis. Overall, LAXIC represents a powerful tool for label-free quantitative phosphoproteomics.

EXPERIMENTAL PROCEDURES

Library Design and Synthesis—Combinatorial libraries of peptides were created as described previously (48) following typical solid phase synthesis and split and mix techniques (49). Reagents were purchased from Midwest Biotech (Indianapolis, IN) except where noted. In this scheme, the C-terminal residue is anchored to phenylacetamidomethyl (PAM) resin beads and the growing peptide chain is constructed by addition of N-tert-butoxycarbonyl (Boc) protected amino acids and 3-(Diethoxy-phosphoryloxy)-3H-benzo[d][1,2,3] triazin-4-one (DEPBT, purchased from National Biochemicals, Twinsburg, OH) as a coupling reagent. For the purpose of synthesizing tryptic-like peptides, the synthesis began with a mixture of PAM resin beads preloaded with arginine or lysine residues. Coupling reactions were performed in separate vessels for each residue with the Boc-

protected amino acid and DEPBT present at 10-fold molar excess. By adding each amino acid in a separate vessel with 10-fold molar excess of reagent, equimolar incorporation of each amino acid at a given position is ensured. To incorporate two amino acids at a given position, beads were dried, divided equally by mass, and redistributed among two reaction vessels beforethe next coupling step. On cleavage and side-chain deprotection with hydrofluoric acid, the retrieved peptides were purified via lyophilization. The efficiency of peptide synthesis was verified using LC-MS data.

DG-75 Cell Culture—The DG75 lymphoma B cells (ATCC) were grown to 50% confluency in RPMI 1640 media supplemented with 10% heat inactivated fetal bovine serum (FBS), 1 mM sodium pyruvate, 100g/ml streptomycin, 100 IU/ml penicillin, and 0.05 mM 2-mercaptoethanol. The cells were washed with phosphate buffered saline (PBS), collected, and frozen at −80 °C for further use. Cells were lysed in lysis buffer containing 50 mM Tris-HCl, pH 7.5, 150 mM NaCl, 5 mM EDTA, 1% Nonidet P-40, 1 mM sodium orthovanadate, 1 × phosphatase inhibitor mixture (Sigma), and 10 mM sodium fluoride for 20 min on ice. The cell debris was cleared by centrifugation at 16,000 × *g* for 10 min. The supernatant containing soluble proteins was collected.

Plant Tissue Culture—*Arabidopsis thaliana* (ecotype Columbia-0) seeds were grown in liquid medium (half-strength murashige and skoog salts and 1.5% sucrose) with 24-h light at room temperature with shaking at ~30 rpm. For the osmotic stress treatment, seedlings of 12-day-old were transferred to fresh medium or medium containing 800 mM mannitol for 30 min. For the ABA treatment, the 12-day-old seedlings were transferred to fresh medium containing 100 μM ABA for 30 min. In parallel, the control sample was incubated in the PBS for the same time period. The control, ABA, and osmotic stress treated seedlings were ground in extract buffer (50 mM Tris, pH 7.5, 200 mM NaCl, and 0.5 mM EDTA). After centrifugation at 12000 × *g* for 30 min, the supernatants were used for further analysis.

Trypsin Digestion—Proteins in cell lysates were denatured in 0.1% RapiGest (Waters, Milford, MA) and reduced with 5 mM dithiothreitol for 30 min at 50 °C. Proteins were alkylated in 15 mM iodoacetamide for 1 h in the dark at room temperature and then digested with proteomics grade trypsin at a 1:100 ratio overnight at 37 °C. The pH was adjusted below 3 and the sample was incubated for 45 min at 37 °C. The sample was centrifuged at 16,000 × *g* to remove RapiGest. The supernatant was collected and desalted with a 100 mg Sep-Pak C18 column (Waters) and dried.

Phosphopeptide Enrichment Using PolyMAC Reagent—The peptide mixture was resuspended in 100 μl of loading buffer (100 mM glycolic acid, 1% trifluroacetic acid, 50% acetonitrile) to which 10nmol of the PolyMAC-Ti reagent (Tymora Analytical. West Lafayette, IN) was added (50). The mixture was incubated for 5 min. The buffer containing 200 μl of 300 mM HEPES at pH 7.7 was added to the mixture to achieve a final pH of 6.3. The solution was transferred to a spin column (Boca Scientific, Boca Raton, FL) containing Affi-Gel Hydrazide beads (Bio-Rad, Hercules, CA) to recover the polyMAC-Ti dendrimers. The column was gently agitated for 10 min and then centrifuged at 2,300 × *g* for 30 s to collect the unbound flow-through. The gel was washed once with 200 μl loading buffer, twice with 100 mM acetic acid, 1% trifluoroacetic acid, 80% acetonitrile, and once with water. The phosphopeptides were eluted from the dendrimers by incubating the gel twice with 100 μl of 400 mM ammonium hydroxide for 5 min. The eluates were collected and dried under vacuum.

Mass Spectrometric Data Acquisition—Peptide samples were dissolved in 8 μl of 0.1% formic acid containing certain amount of internal standard peptide library and injected into an Eksigent NanoLC Ultra 2D HPLC system. The reverse phase C18 was performed using an in-house C18 capillary column packed with 5 μm C18 Magic beads resin (Michrom; 75 μm i.d. and 30 cm of bed length). The mobile phase buffer consisted of 0.1% formic acid in ultra-pure water with an eluting buffer of 0.1% formic acid (Buffer A) in 100% CH_3CN (Buffer B) run over a linear gradient of 60 mins with a flow rate of 300 nl/min. The electrospray ionization emitter tip was generated on the prepacked column with a laser puller (Model P-2000, Sutter Instrument Co.). The Eksigent Ultra2D HPLC system was coupled online with a high resolution hybrid duel-cell linear ion trap Orbitrap mass spectrometer (LTQ-Orbitrap Velos; Thermo Fisher). The mass spectrometer was operated in the data-dependent mode in which a full-scan MS (from *m/z* 300–1700 with the resolution of 60,000 at *m/z* 400) was followed by ten MS/MS scans of the most abundant ions. Ions with charge state of +1 were excluded. The mass exclusion time was 15 s.

Peptide Matching and Protein Identification—The LTQ-Orbitrap raw files were searched directly against *Homo sapiens* (93,289 entries; human International Protein Index (IPI) v.3.83) or *Arabidopsis thaliana* database (39,678 entries; *Arabidopsis* International Protein Index (IPI) v.3.84) with no redundant entries using SEQUEST algorithm on Proteome Discoverer (Version 1.3; Thermo Fisher). Proteome Discoverer created DTA files from the raw data with minimum ion threshold of 15 and absolute intensity threshold of 50. Peptide precursor mass tolerance was set at 10 ppm, and MS/MS tolerance was set at 0.8 Da. Search criteria included a static modification of cysteine residues of +57.0214 Da and a variable modifications of +15.9949 Da to include potential oxidation of methionine residues and a modification of +79.996 Da on serine, threonine, or tyrosine for the identification of sites of phosphorylation. Searches were performed with full tryptic digestion and allowed a maximum of two missed cleavages on the peptides analyzed from the sequence database. False discovery rates (FDR) were set for 1% for each analysis. Proteome Discoverer generates a reverse "decoy" database from the same protein database, and any peptide passing the initial filtering parameters that were derived from this decoy database is defined as a false positive. The minimum cross-correlation factor (Xcorr) filter was re-adjusted for each individual charge state separately in order to optimally meet the predetermined target FDR of 1% based on the number of random false-positive matches from the reversed "decoy" database. The number of unique phosphopeptides identified were then manually counted and compared. Phosphorylation site localization from CID mass spectra was determined by PhosphoRS scores and only one phosphorylation site was counted using the top scored phosphopeptide for any phosphopeptide with potentially ambiguous phosphorylation sites.

Annotated sequence spectra supporting identification of phosphorylated peptides associated with this manuscript can be downloaded from ProteomeCommons.org Tranche (https://proteomecommons.org/tranche) using the following hash: HIBTRMQhBK5H2mf7-PmhDSBGZHwEJW3/ciGRL2JCzBkklxvZNEBYPv6kuNIj+jaMOPw-f5g3pS2ocYWJWWGMOxQwupLyEAAAAAAAACKw==.

Ion Intensity Based Label-free Quantitation—Peak detection, alignment are performed by TOPPAS (51) using MapAlignerPoseClustering node. The intensity ratio of aligned peak I_1 and I_2 in two samples to be compared was calculated as Ratio = I_1/I_2. The peak intensity ratios of all identified library peptides were used as a set of normalization factors for the estimation of abundance ratio of sample peptides. Specifically, for a peptide ion identified at retention time *x*, we compute a weighted normalization factor based on two identified library peptides with the closest retention time to *x* (denoted *as* i and *j*, respectively):

$$NF_x = NF_i \cdot \left|\frac{x - j}{i - j}\right| + NF_j \cdot \left|\frac{x - i}{i - j}\right| \quad (1)$$

TABLE I
Peptide libraries used in this study. Residues in parenthesis indicate that either of these two options is present in a given peptide

Library	Sequence	# Peptides	Eisenberg[a] Hydrophobicity Range
AT11A	**(A/Y)(T/Q)E(V/H)GS(T/N)P(G/S)ER**	**32**	**−5.18 to −2.62**
AT11D	**A(T/Q)(I/E)V(L/G)P(G/T)(L/S)(F/S)(I/E)K**	**128**	**−2.85 to 2.73**
ER12A	**(F/G)(V/N)(A/D)(S/I)(L/K)(GPI/ETY)(F/L)(T/Q)(S/A)(K/R)**	**1024**	**−5.52 to 3.06**
BB11A[b]	**(A/Y)(T/Q)(E/A/I)(H/V)(L/G)(S/P)(T/N)(L/P)(S/G/F)(E/I)(K/R)**	**4608**	**−5.14 to 2.39**

[a] Eisenberg, D.; Schwarz, E.; Komarony, M.; Wall, R. (1984) Amino acid scale: Normalized consensus hydrophobicity scale. *J. Mol. Biol.* 179, 125–142.
[b] Bohrer, B. C., Li, Y. F., Reilly, J. P., Clemmer, D. E., DiMarchi, R. D., Radivojac, P., Tang, H. X., and Arnold, R. J. (2010) Combinatorial libraries of synthetic peptides as a model for shotgun proteomics. *Anal Chem* 82, 6559–6568.

where *NFi* and *NFj* represent the peak intensity ratios of the two identified library peptides eluting at retention time *i* and *j*, respectively.

Finally, for a nonlibrary peptide that were identified multiple times in a LC-MS/MS experiment, we computed its quantity ratio between two samples as the geometric mean of normalized intensity ratios among all quantified ions of the same peptide:

$$\text{PepRatio} = \sqrt[N_m]{\prod_{i=1}^{N_m} \text{PeakRatio}_i} \quad (2)$$

Statistical Analysis—Statistical analyses including one sample *t* test, two sample paired *t* test, Wilcoxon Signed Rank Test, one-way analysis of variance (ANOVA) were performed at the significance level of p value < 0.01 except further notice. For the box-plot visualization, mean, first and third quartiles were presented as three horizontal lines in the box, 5 and 95% percentiles were shown as upper and lower bounds, and outliers were marked as dots.

In the regression model, square of Pearson's correlation coefficient (R^2), slopes and intercepts of linear regression functions between phosphopeptide ion intensities and percentage of plant cell extract were calculated by Microsoft Excel. Correlations were considered statistically significant at $R^2 >= 0.525$, 0.681, or 0.930 ($p < 0.05$ when five, four, or three data points were used to construct the linear regression function, respectively). The accuracy of each phosphopeptide can be obtained as below.

$$Acc = \frac{I_{cal} - I_{theo}}{I_{cal}} \times 100\% \quad (3)$$

$$\%Acc = \frac{\sum_{i=1}^{n} Acc_i}{n} \times 100\% \quad (4)$$

Where I_{cal} is the calculated relative LAXIC ratio (each data point is normalized to maximum LAXIC ratio among five proportions) of the phosphopeptide and I_{theo} is the theoretical ratio obtained using the linear regression function. *Acc* is the accuracy of each phosphopeptide in one dilution sample and *%Acc* is the mean percentage accuracy (*%Acc*) from each dilution. Coefficient of variation (CV) was calculated as S.D./mean × 100. FDR was based on the number of false-positive hits for the library peptides which have theoretical equal amount among samples.

RESULTS

Design and Characterization of Synthetic Peptide Libraries for Phosphoproteomics—To achieve accurate quantitation using the LAXIC approach, a well-designed peptide library is required based on the following criteria: (1) Peptides should distribute along the whole chromatogram and cover a wide range of retention time. (2) Number and amount of peptides should be appropriate for LC-MS analysis for accurate quantitation while not affecting the sensitivity of analysis. (3) Peptide sequences that have amino acids with potential modifications (*e.g.* Cys, Met) during the sample preparation should be avoided. Accordingly, we used one previously described (48) and four newly designed libraries to determine the library appropriate for the study. Library BB11A, containing 4608 unique sequences, was part of a previous study and served as a model of a complex proteome sample. Library AT11A was designed as a much smaller library (32 sequences) and intended to model the hydrophilic nature of many phosphopeptides (supplemental Fig. S1, upper panel). Library AT11D containing128 unique sequences was designed to model a wider range of hydrophobicity typical of nonphosphorylated peptides and provide options in terms of complexity (supplemental Fig. S1, lower panel). The libraries were generated using a combinatorial synthesis technique and the detail sequence design was shown in Table I.

Next step, we investigated the effects of library size (number of unique sequences in the library) and amount of peptide library on the analysis of complex samples. It is conceivable that the calibration will not be accurate enough if the library is too small and cannot sufficiently cover the whole chromatogram evenly. Real sample signals, on the other hand, may be suppressed by large amount of spike-in library peptides. To examine the exogenous suppression effect by the library peptides, a titration experiment was carried out using a typical phosphopeptide sample prepared from the enrichment of 100 μg of whole cell extracts with the peptide library BB11A in different amounts. We compared the numbers of identified phosphopeptides and library peptides as a function of amount of spiked peptide library (Fig. 2*A*). As expected, excess amounts of library peptides as internal standards will affect the phosphopeptide identification, likely because of overwhelming of mass spectrometer's scanning speed and/or ion suppression effect. With a peptide library (AT11A+AT11D) at appropriate size, we did not observe the interference on phosphopeptide detection in terms of the identification and quantification (supplemental Fig. S2*A*). Two folds difference in spiked library amount did not cause detectable bias of phosphopeptides quantitation in two independent experiments,

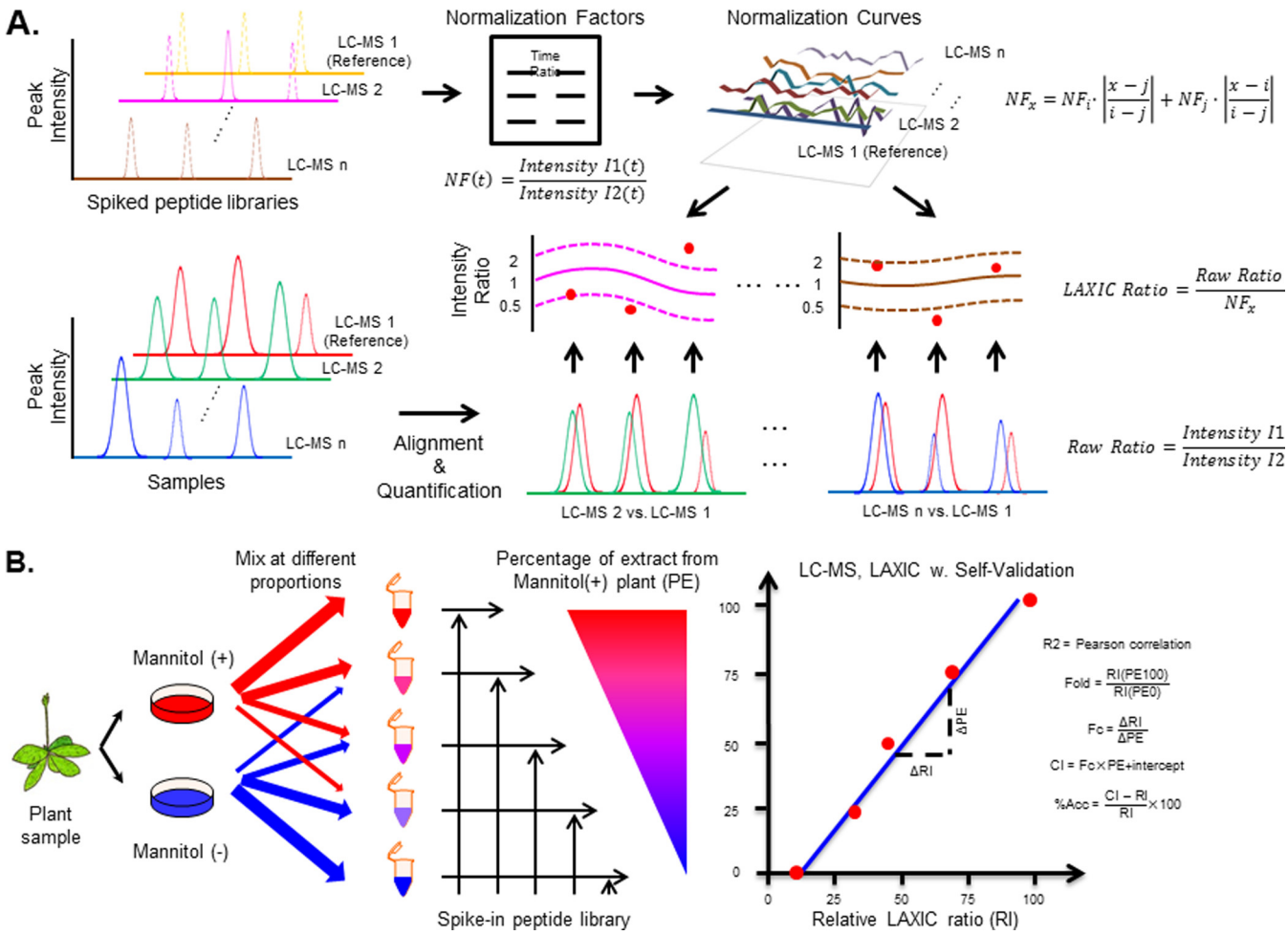

FIG. 1. **Work flow for the LAXIC strategy to quantify the phosphorylation change in response to osmotic stress.** *A*, Schematic representation of the LAXIC algorithm. First, all the chromatographic peaks were aligned and the ratios were calculated. Second, the normalization factors which equal to ratios of library peptide peaks between MS runs were chosen to construct normalization curve. Third, sample peptide peak ratios were normalized against predicted normalization factor corresponding to certain retention time. *B*, Schematic representation of quantitative phosphoproteomics. Plants either treated with mannitol or PBS were lysed and mixed proportionally at first. Following peptide digestion and enrichment, phosphopeptides were identified and further quantified through LAXIC incorporated with self-validating process using thelinear regression model to analyze the fold change (fold), linearity (R^2) and accuracy (%Acc).

and the ratio of two identical samples held at 1:1 (Wilcoxon Signed Rank Test, theoretical median = 1).

Given the purpose of utilizing internal standards to monitor the LC-MS condition, the retention time range of library peptides should be no smaller than it would be for real sample. In addition, an even distribution of spike-in peptides across the chromatogram would be ideal, as a large gap between two internal standards can affect the accuracy of local normalization. AT11D, which is composed of 128 peptides, is derived from the large library BB11A containing 4608 peptides based on the retention time coverage. Furthermore, the hydrophilic library AT11A was included to cover phosphopeptides that may elute early in on the reverse phase chromatography. For the current libraries AT11A and AT11D, the maximum gap between two library peptides is about 1.5 min in a 60 min LC gradient (Detail chromatographic settings are in the Experimental Procedure). The overall widths and ranges of distributions for the combined peptide libraries AT11A&AT11D are in good agreement with the human phosphoproteome (Fig. 2*B*). Together, the full retention coverage and relatively uniform distribution of library peptides guarantee that phosphopeptides eluted at a given time could be monitored by at least two closely surrounding library peptides.

Characterization of LAXIC Quantitation Algorithm—To evaluate the quantitation accuracy of LAXIC, we compared the mean ratio of identical standard peptide mixtures spiked with the peptide libraries AT11AD. Corrected LAXIC ratios were closer to one when compared with raw ratios (Wilcoxon Signed Rank Test, theoretical median = 1, p value of raw ratio < 0.0001 but equals to 0.028 after normalization) (supplemental Fig. S2*B*). The normalization process was statistically significant with the p value of two sample paired t test

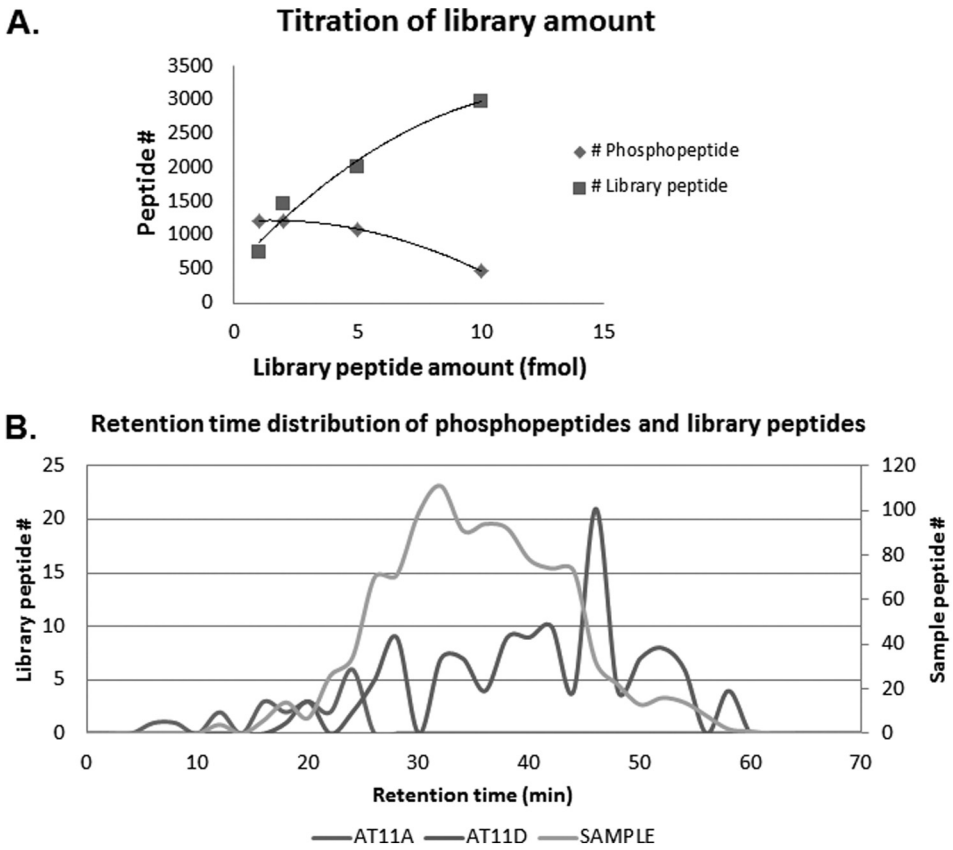

FIG. 2. **LC-MS characterization of synthetic peptide library.** *A,* Number of phosphopeptides identified in DG75 cell lysate *versus* diverse amounts of peptide library. *B*, Histogram of chromatographic distribution of phosphopeptides enriched from DG75 cell lysate and peptides from library AT11A/D.

below 0.01, whereas standard deviation of log ratios was similar before and after normalization (0.27 in replicate 1 and 0.31 in replicate 2, respectively), indicating the normalization probably corrected the system errors without disturbing the sample variance. Similarly, LAXIC led to more accurate quantitation of identical phosphopeptides samples that were isolated directly from human B lymphocyte DG75 cells (supplemental Fig. S3*A*, S3*B*). As shown in supplemental Fig. S3*C*, a pattern of up-shifted ratio at the late retention time indicated a potential system bias for two identical LC-MS runs. This bias can be corrected by our prior knowledge of equal loading peptide libraries. On the other hand, there was no significant pattern for the variation of ratios by plotting the delta log ratios against the retention time (supplemental Fig. S3*D*), implying the homogenous performance of library peptides across the LC gradient. Together, the various ratios of internal standards across the whole chromatogram indicated that it is less accurate to use one or a few peptides as the internal control, or one single normalization method based on single value in the global scale. By computing the ratios of individual phosphopeptides, we observed significant difference among three quantification process, no normalization, global normalization by total ion current (TIC), and local normalization by LAXIC (One-way ANOVA, p value < 0.01) (supplemental Fig. S3*E*). Moreover, higher quantitation accuracy of LAXIC was interrogated by comparison with the total intensity normalization method using Wilcoxon signed rank test.

To further evaluate the effect of adding synthetic peptide library into real samples, we spiked different amounts of library peptides into a complex phosphopeptide sample and then analyzed by LC-MS. Identical phosphopeptides were quantified when the absolute amount of samples was 25 μg, 50 μg, and 100 μg lysate, respectively (supplemental Fig. S4*A*). Interestingly, we found the LAXIC normalization showed the largest correction when the sample amount was increased. The two sample paired t test was performed to compare raw ratio *versus* LAXIC ratio with p value of 0.49 for 25 μg lysate, but less than 0.01 for 50 μg and 100 μg lysate. We reasoned that it was probably because of the greater complexity in larger amount of samples, requiring quantification adjustment to remove the suppression effects. Furthermore, supplemental Fig. S4*B* with one sample t test showed that twofold change of real sample amount was consistently better correlated with LAXIC ratio 2 on average.

The dynamic range of LAXIC quantitation was investigated based on a titration experiment in which a larger library, ER12A (Table I), with around 1000 synthetic peptides was used to mimic a biological sample. In this experiment, the

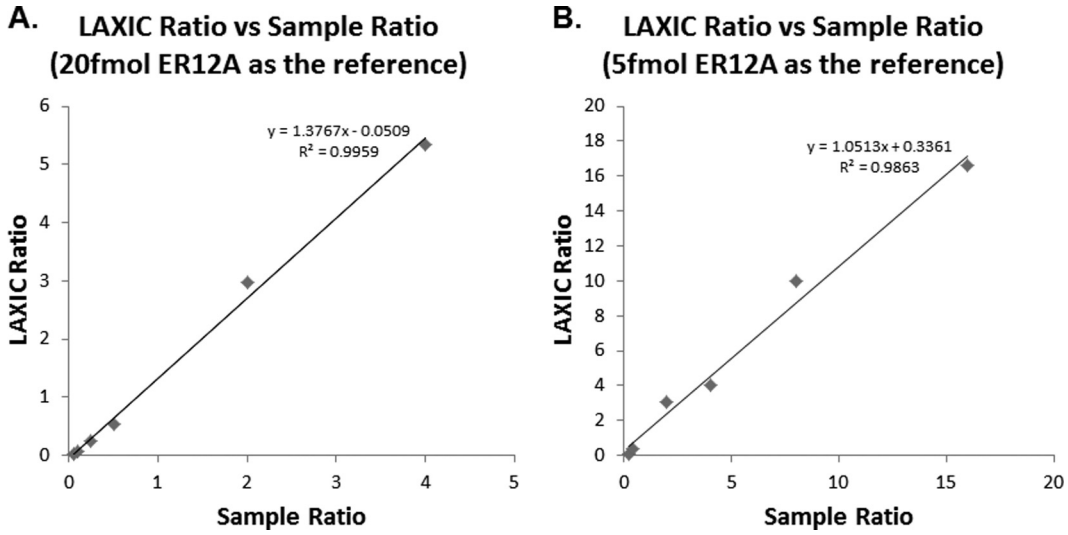

FIG. 3. **Dot-plot of LAXIC ratio *versus* actual sample ratio, showing the dynamic range of LAXIC quantification.** *A*, 20 fmol peptide library ER12A as the reference. *B*, 5 fmol peptide library ER12A as the reference.

ER12A library was used in a series of amount, 1, 2, 5, 10, 20, 40, 80, and 160 fmol, and equal amount of peptide library AT11AD was spiked into each sample (Fig. 3). A linear correlation of LAXIC ratio *versus* sample ratio was retained from 0.05 to 16 using 5fmol and 20 fmol ER12A as the references, while the LAXIC ratio of 160 fmol ER12A was deviated from the actual sample ratio. Failure to quantify such large ratio change was likely due to strong suppression of sample ion to the spike-in library, because the assumption of LAXIC requires high consistency of the spike-in library. In this case, a ~16-fold ratio appears to be a safe linear dynamic range for LAXIC quantitation.

Application of LAXIC to Complex Plant Cell Extracts—Metabolic labeling using stable isotope labeling by amino acids in cell culture (SILAC) can be used for cell culture, but it is not effective for autotrophic organisms such as plants or bacteria (52). Label-free quantitation could provide an alternative method to study quantitative proteomics in plants without introducing extra steps. To test whether the LAXIC technique is applicable for complex biological samples, plant samples with ABA treatments were examined. ABA is a hormone that controls seed dormancy, germination, and plant response to environmental stresses through phosphorylation signaling. This model is one of the well-studied signaling pathways in plants and Sussman and coworkers have carried out a comprehensive study on phosphoproteome response to ABA treatment in *Arabidopsis* using isotope labeling quantitative mass spectrometry approach (53). In contrast to the ^{15}N isotope labeling in their experiment, we compared the phosphorylation change between 30 min ABA treatment and control in wild-type *Arabidopsis* using a label-free approach. In a single experiment, a total of 1562 phosphopeptides were quantified based on the LAXIC method, corresponding to about 70% coverage of the total identified phosphopeptides from two samples (supplemental Table S1). The mean ratios (ABA *versus* control) for all phosphopeptides before and after LAXIC processing were 0.7 and 0.99 respectively (Fig. 4*A*, 4*B*). LAXIC normalization helped correct the sample variation among LC-MS runs, confirming the previous report that ABA treatment did not perturbed the global phosphorylation level (53). In addition, comparing the normalization methods to correct background variations (Fig. 4*C*), the LAXIC outperformed the library based global normalization and achieved similar accuracy with total intensity normalization, in terms of the deviation of mean ratios between experimental and theoretical value (Fig. 4*D*). To facilitate visual interpretation of all quantified phosphopeptides, a box-and-whisker plot was provided to depict the distribution of ratios found in each sample (details of the box-plot description were in the Experimental Procedure). Among those 50 reported phosphopeptides that have significant change response to ABA (53), 26 of them were identified in our one run experiment (Supplemental Table S2). Moreover, 21 out of those 26 phosphopeptides in our experiment corresponded to the same phosphorylation changes as reported previously. Based on these data, both the accuracy and sensitivity of LAXIC were confirmed for complex biological samples.

Plant Phosphorylation Signaling in Response to Osmotic Stress—Osmotic stress associated with drought or salinity is a major factor that limits plant productivity. It activates signaling pathways that lead to rapid changes in gene expression and metabolism, some of which presumably help plants cope with the stress (45). However, the phosphorylation regulation toward osmotic stress has remained unclear. Previous studies indicated that osmotic stress caused accumulation of the hormone ABA and several osmosis-regulated kinases, and it was intuitive to study plant phosphoproteomics in regards to this external stress. In order to achieve high accuracy

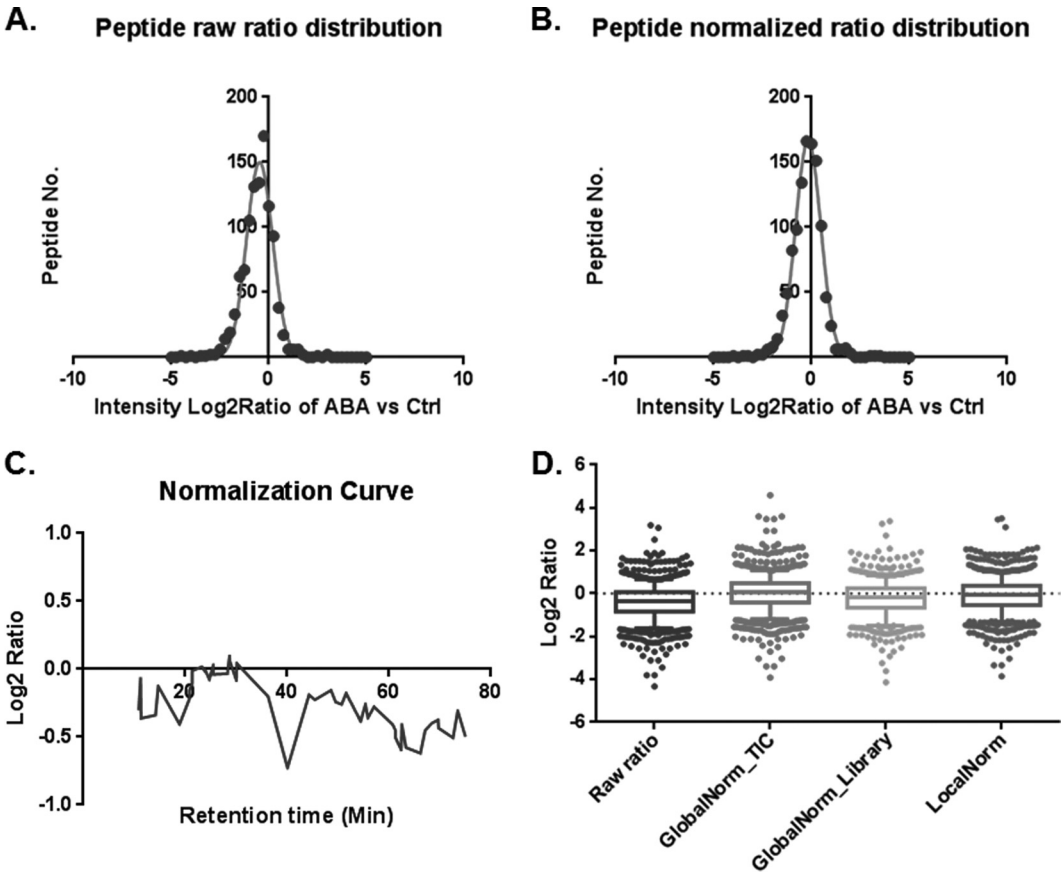

FIG. 4. **Representative example of LAXIC performance for complex plant phosphoproteome.** *A* and *B*, Distribution of phosphopeptide ratios before and after LAXIC normalization. *C*, Normalization curve depicted by ratios of library peptide intensities through chromatogram. *D*, Box-plot for quantitative comparison of phosphopeptides between ABA(+) and control plant, generated by different normalization processes, including no normalization, global normalization by total peptide intensity, global normalization by average peptide library intensity, and local normalization by peptide library.

and confidence in label-free quantitation data, we combined the label free LAXIC quantitation with a self-validating method (47) to study phosphorylation changes in *Arabidopsis* in response to osmotic stress. Because the overall low stoichiometry of phosphopeptides, current data dependent acquisition based LC-MS experiments usually yield few spectra of phosphopeptides per sample, leading to the difficulty of assessing the analytically well behaved phosphopeptides out of thousands of total identifications (10, 54, 55). By combining the self-validating method developed by Casado and Cutillas (47) and the LAXIC approach, we simultaneously evaluated the precision and accuracy of large quantitative phosphoproteomics data generated from complex biological samples.

Based on this strategy (Fig. 1*B*), plants treated with either mannitol or PBS (as control) was lysed and mixed proportionally. In our experimental design, given the same amount of treatment and control plants (protein weight), 0, 25, 50, 75, 100% of mannitol treated plants were mixed with 100, 75, 50, 25, 0% of control plants to generate five distinctive samples in which the quantities of each identical phosphopeptides have intrinsic linear relations. Following trypsin digestion and phosphopeptide enrichment, phosphopeptides from the five samples were spiked in with equal amount of library AT11A&D and individually identified by LC-MS/MS and quantified by LC-MS through LAXIC process (Fig. 1*B*). The experiment was performed in two replicates. Using the 50% mannitol/50% control sample as the reference, the LAXIC ratios of other 4 samples compared with that were assigned. Those 5 LAXIC ratios, including the constant 1 for the 50% data point, were again normalized to their maximum. Lastly, the normalized LAXIC ratios were used for the regression model. A linear regression function was applied to measure the linearity and accuracy of each quantified phosphopeptide. The linearity was calculated by the Pearson's correlation coefficients (R^2) and the accuracy was determined by the residual of LAXIC ratio *versus* predicted ratio calculated by the regression model (Fig. 1*B*).

We qualitatively identified a total of 2223 unique phosphosites, representing 2027 phosphopeptides on 1034 proteins (supplemental Table S3, S4). The contributions of pS, pT, and pY were 88.3%, 9.8%, and 1.9% respectively, supporting the previous notion about the phosphorylation pattern in *Arabi-*

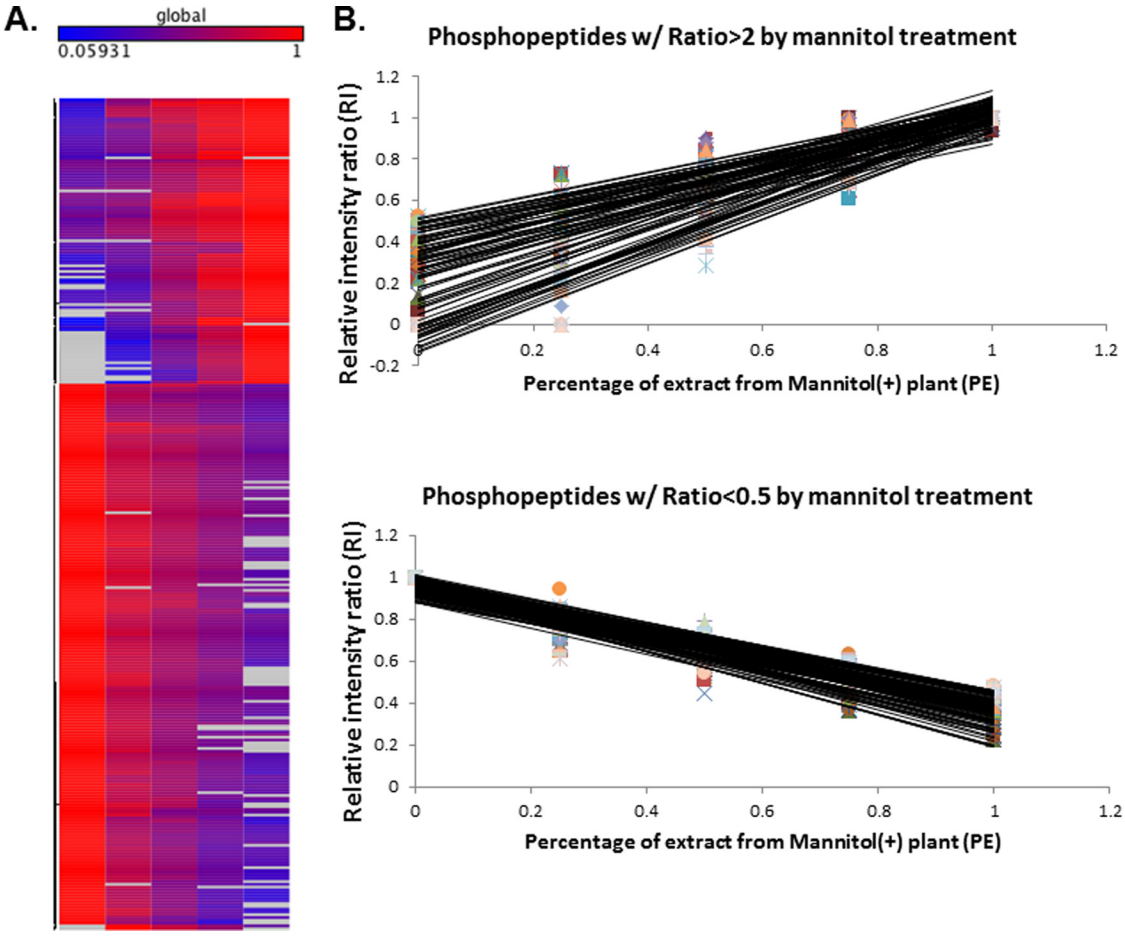

FIG. 5. **Phosphopeptides differentially regulated by mannitol treatment.** *A*, A heat map of normalized phosphopeptide intensities as a function of the proportion of cells in the mixture. *B*, Representative examples of regulated phosphorylated peptides by mannitol treatment.

dopsis (30). Altogether, 1850 phosphopeptides were quantified across the two types of samples, and relative phosphopeptide intensities across five mixture samples were shown in the heat map (Fig. 5*A*). The intensity of each peptide was normalized to the highest intensity among the columns in each row. Quantifications were considered accurate when mean accuracy (%Acc) $< 30\%$, linear when Pearson's correlation coefficient (R^2) > 0.805, 0.924, 0.997 for 5, 4, or 3 data points respectively, and precise when coefficient of variance (CV) $< 50\%$ (47). R^2 values were chosen based on their statistical significance and %Acc and CV cutoff values were set arbitrarily. With the twofold change cutoff, the FDR based on library peptide calculation was less than 1%. As a result, we chose twofold as the criteria to consider significance of phosphorylation change. Taken together, 442 phosphopeptides were quantified with adequate accuracy (%Acc$<$30%), linearity (p value of R^2 $<$0.01), and precision (CV $<$ 50%). 134 phosphopeptides of those showed twofold increase in mannitol treatment plants relative to control, whereas 221 phosphopeptides showed twofold decrease (Fig. 5*B*). Some weak statistical phosphopeptides with only two data points out of five were counted as twofold change peptides when (1) Two data points both have interpretable ratio. (2) CV of each point is less than 0.5. (3) Ratio of mannitol treated or control sample to 50% mixture is more than 1.414. Forty-five significant phosphopeptides in this category were listed in supplemental Fig. S5 and supplemental Table S5.

Besides the self-validating quantitative result, pairwise quantitation comparison was performed for the mannitol *versus* PBS treated plant samples as well. A total of 185 phosphopeptides were identified as twofold change comparing mannitol (+) *versus* (−) with adequate precision (CV$<$50%). From this result, combined with self-validating quantified phosphopeptides above, there were 169 phosphopeptides up-regulated and 299 down-regulated by osmotic stress (Fig. 6, supplemental Table S6, S7). A common question related to quantitative phosphoproteomics is that whether the measured phosphorylation changes result from changes in protein expression. We therefore closely examined all quantified phosphopeptides. Among them, 202 unique proteins had more than 1 phosphopeptide. The phosphopeptide ratios in 104 proteins showed similar trend of increase or decrease, whereas 98 other proteins show distinct trend in their phosphopeptides. The results indicated that there were significant

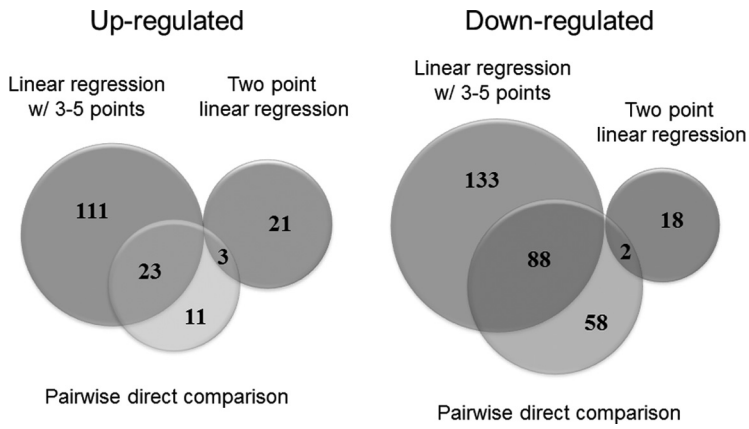

FIG. 6. **Differentially phosphorylated peptides identified in comparison of mannitol treated plant and control.** Venn diagram illustrated the overlap by three quantitation categories.

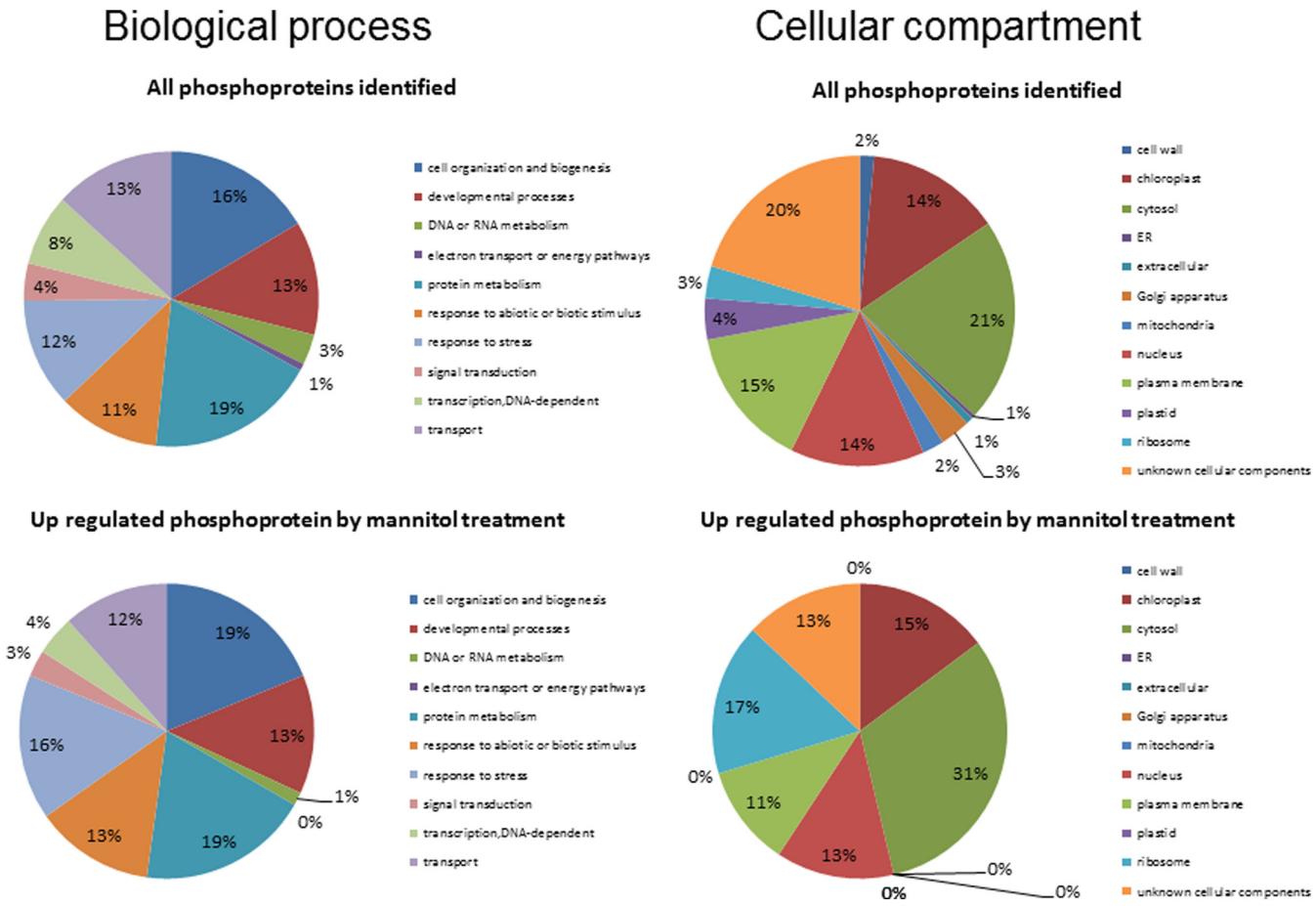

FIG. 7. **Distribution of the phosphoproteins based on GO analysis, including biological process (*Left*) and cellular component (*Right*).** *Top* panel is the distribution of all phosphoproteins identified, while *bottom* panel is the distribution of differentially phosphorylated proteins containing increase signal in mannitol(+) plant.

phosphorylation changes independent of protein abundance but it did not rule out the effect of the protein expression change on measured phosphorylation change (56).

GO analysis was conducted for all the phosphoproteins identified in the context of their biological process, molecular function, and cellular compartment (supplemental Table S8). Proteins with twofold phosphorylation changes in response to osmosis stress were annotated using Gene Ontology (GO) through The *Arabidopsis* Information Resource (TAIR). The plant treated with mannitol showed greater phosphorylation on "stress response" and "response to abiotic or biotic stimulus" than overall background (Fig. 7). These observations are consistent with the perception that mannitol treatment can mimic osmotic stress for plant biology (57). It is also notewor-

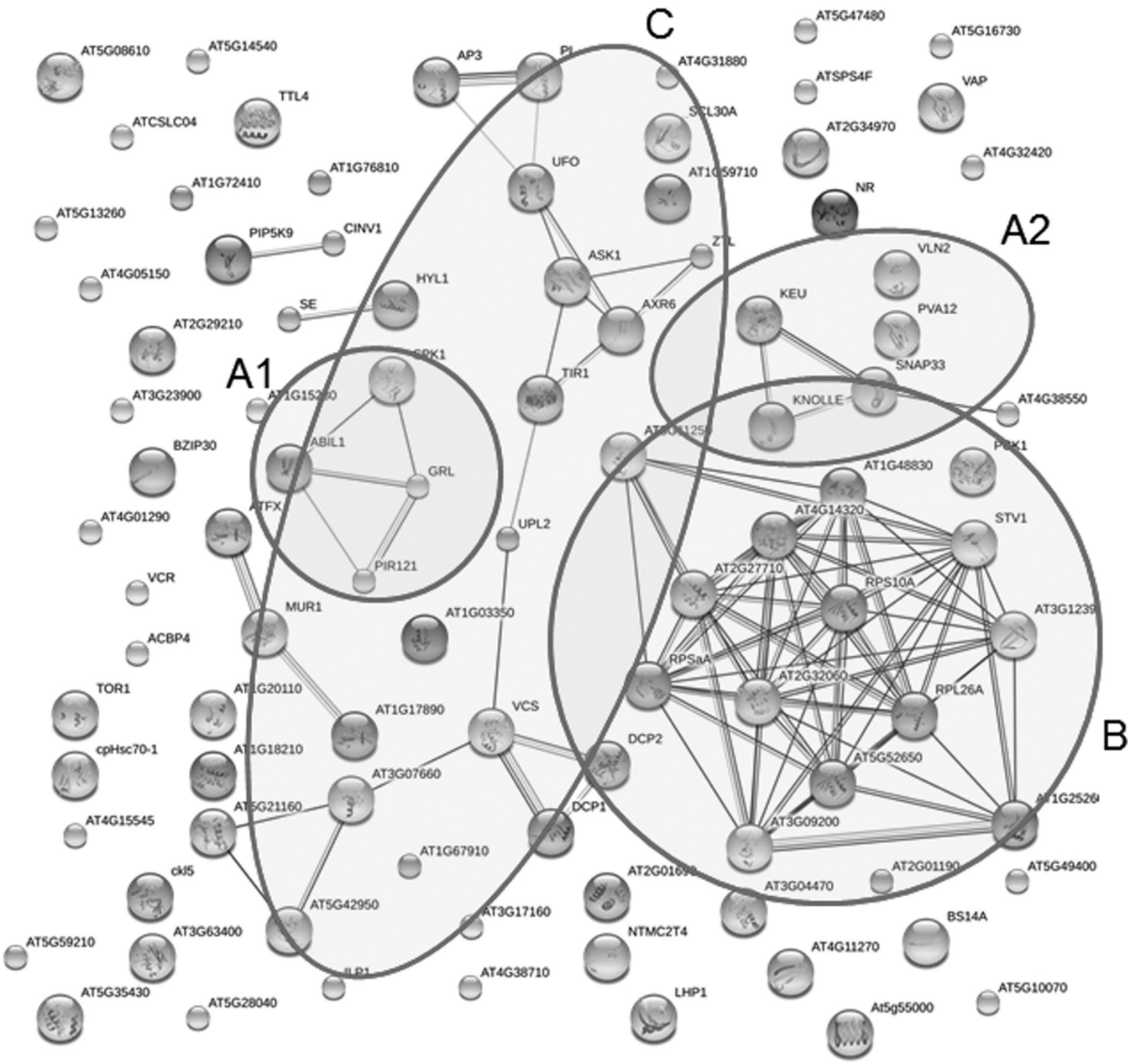

FIG. 8. **Interaction networks of the regulated phosphoproteins.** STRING system (http://string.embl.de) was used to map the network by known and predicted interactions. Different types of evidence for the associations were represented by different colors. Cytoskeleton dynamics (*A*), translation (*B*) and post-translational modification (*C*) were three major clusters based on the associations of the proteins.

thy to observe that "transport" related phosphorylation is down regulated for mannitol treatment, suggesting a potential strategy for stress response in plant.

To better understand the network among those phosphoproteins that are regulated by osmotic stress, a protein-protein interaction network was derived from experimental results, literature mining and computation prediction using the STRING system (58). Three major clusters were derived from the phosphoproteins up-regulated by mannitol treatment (Fig. 8). The first cluster involved in cytoskeleton dynamics is composed of six proteins involved in cytokinesis, WAVE complex constitution and microtubule association. The second cluster consists of 11 proteins, 10 of which are ribosomal proteins, indicating that translation process is highly regulated by phosphorylation. The third cluster contains proteins processing in post-translational modification, such as SnRK in the phosphorylation signaling and AXR6 in the ubiquitination process.

The sequence consensus of phosphopeptide motifs reflected the kinase-specific regulation of substrates phosphorylation and the identity of the corresponding kinases. Eleven

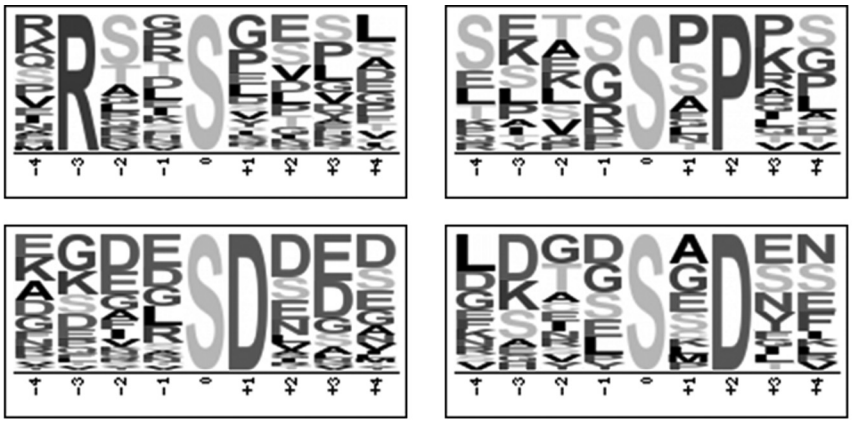

#	Motif	Motif Score	Foreground Matches	Foreground Size	Background Matches	Background Size	Fold Increase
1.	.R..s....	10.72	35	172	54410	988357	3.70
2.	....sD...	10.74	30	137	48468	933947	4.22
3.	....s.P..	4.23	17	107	47632	885479	2.95
4.	....s.D..	4.03	15	90	45249	837847	3.09

FIG. 9. **Significantly enriched phosphorylation motifs from up-regulated phosphopeptides by Motif-X analysis.** The IPI *Arabidopsis* protein database was used as the background database to normalize the score against random peptide sequences. Motifs 1, SnRK2 kinase family motif; Motif 2, CKII motif; Motif 3 and 4, unknown phosphorylation motifs.

significantly enriched phosphorylation motifs were extracted from phosphopeptide data sets and identified using the Motif-X (59) algorithm (Fig. 9). Using the *Arabidopsis* proteome as the background, a list of consensus motifs in our phosphopeptide data sets were enriched in mannitol treatment plant (p value < 0.000001), including some known kinases involved in osmotic stress, *e.g.* RXXpS/pT for SnRK2 kinase family and pSD for CK2 kinase (60). These two kinase families were both involved in ABA pathway as well, illustrating that ABA plays an essential role in such abiotic stress (61). Other motifs, like pSXP and pSXD have not yet been assigned to any specific kinases. On the other hand, some motifs such as pSP, pSDX[D/E], pSX[D/E], and pSXXEE were enriched in the down regulated phosphopeptides by mannitol treatment (supplemental Fig. S6), suggesting that the cyclin dependent kinase (CDK) family, mitogen activated protein kinase (MAPK), Glycogen synthase kinase 3 (GSK3), and casein kinase II (CK II) may be suppressed in the response to osmotic stress.

Phosphorylation Regulation of SnRK2 Kinases and ABA-responsive Genes—It has been reported that nine out of the ten SnRK2s can be activated by mannitol or NaCl treatment (43). In our result, we found that the phosphorylation of SnRK2.1 could be induced (2.2 folds, $p < 0.05$) after 30 min mannitol treatment. A peptide STVGTPAYIAPEVLSR, which represents the conserved motif of SnRK2.1, SnRK2.4, SnRK2.5, SnRK2.10, was only phosphorylated under the osmotic stress treatment. As pointed out above, the RXXpS/pT motif was detected in the osmotic stress up-regulated phosphopeptide list (Fig. 9). This motif is enriched in the potential substrates of SnRK2.10 (62). Those proteins containing RXXpT/pS motif may represent the substrate candidates of osmotic stress activated by SnRK2. All these results strongly suggest a critical role of SnRK2s and its target protein in osmotic stress signaling. Interestingly, compared with the recent work (53), several ABA induced phosphopeptides also were present in our list, including a bZIP family transcription factor, dyanmin 2B and a GYF domain containing protein. In contrast, the phosphorylation of PP2C and an IQ-DOMAIN 32 protein was suppressed by both ABA and osmotic stress treatment (supplemental Table S7, S8). It has been well characterized that osmotic stress can trigger the accumulation of ABA (61), and both ABA and osmotic stress can activate SnRK2s. The high overlap between ABA and mannitol activated phosphorylation indicated that they may share the same kinase pathway.

Phosphorylation Regulation in Osmotic Stress Responsive Genes—The phosphorylation of several well-characterized stress-related proteins is up-regulated by osmotic stress. CINV1 encodes a neutral invertase and under mannitol treatment, the growth of lateral root in wild-type is totally inhibited, whereas the growth of mutant *civn1* is less sensitive (63). Though there was no direct evidence indicating that CINV1 is regulated by phosphorylation, the presence of CINV1 in our result indicated its potential post-translational regulation under osmotic stress treatment. CLB1, a calcium-dependent lipid-binding transcription factor, can act as a negative regulator in osmotic stress. Deficiency of CLB1 increases NaCl tolerance in *clb1* mutant (64). Tudor-SN is a RNA binding

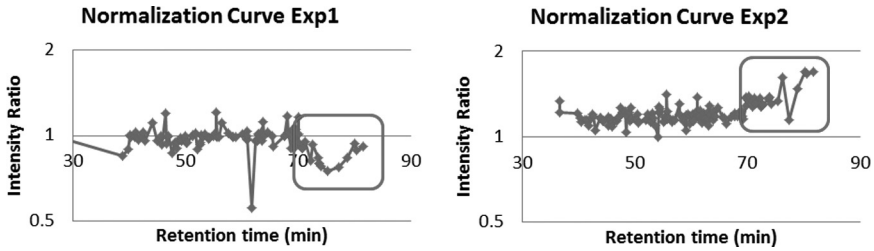

FIG. 10. **Representative normalization curves for complex plant phosphoproteome from two identical experiments.**

TABLE II

Comparison of normalization methods for some representative phosphopeptides. RT, retention time; Raw, raw ratio of specific peptide between duplicates; Global, normalized peptide ratio with the global normalization factor calculated by overall internal standards; Local, normalized peptide ratio with the local normalization factors calculated by distinct internal standards; Change, ratio difference between local and global normalization methods. Note: lower-case residues in peptide sequences have phosphorylation

Sequence	LC-MS 1					LC-MS 2				
	RT [min]	Raw	Global	Local	Change	RT [min]	Raw	Global	Local	Change
SFLLDDASDGNEsGTEEDQSAFMK	70.36	1.2	1.25	1.31	9%	70.6	2.34	2.12	1.79	23%
VEEKEEsDEEDYGGDFGLFDEE	71.62	0.29	0.3	0.35	19%	71.86	0.63	0.57	0.46	28%
AGsLEGLEFDFK	74.23	0.79	0.82	1.02	30%	74.48	1.34	1.21	1.02	24%
KGYtSDEELEELDSPLTSIVDK	76.8	0.5	0.51	0.65	30%	76.9	1.34	1.21	1.04	22%
AFFDsADWALGK	77.07	0.71	0.73	0.91	29%	77.22	1.44	1.3	1.24	14%
KKEEsEEEEGDFGFDLFG	78.05	0.95	0.99	1.17	22%	78.56	1.93	1.74	1.38	28%
AsSGPDLSEIPNPADFPVIR	81.58	0.39	0.4	0.42	10%	81.35	1.32	1.19	0.78	41%
KKDEPAEEsDGDLGFGLFD	83.66	0.96	0.99	1.02	7%	84.31	2.41	2.18	1.59	34%

protein, and is important for RNA stability of its targets in plant. The germination and growth of double mutant *tsn1 tsn2* is hypersensitive to high salinity stress (65). Interestingly, SNAP33 (66) and CRT1a (67, 68), which are involved in plant immunity, were also phosphorylated under osmotic stress. CRT1a has been recognized to increase phosphorylation when PP2A is inhibited (69). This phosphorylation event implied potential cross-talks between abiotic and biotic response. We also noticed that there were several RNA binding proteins, Proline-rich proteins and G-proteins phosphorylated under osmotic stress, though their functions in osmotic stress response have not been characterized.

DISCUSSION

At present, MS-based quantitative phosphoproteomics is one of the most powerful tools for profiling signaling networks on a global scale. Label-free quantitative phosphoproteomics circumvents shortcomings inherent to labeling strategies, including the difficulty of comparing large sample numbers, and their cumbersome and costly nature. However, although in principle attractive, it is known to have less than satisfactory reproducibility and accuracy. We reasoned that inconsistencies are due largely to parallel experimental processes, varied amount of sample injection and ion suppression effect. The latter two factors are considered to be the environmental variation during LC-MS procedure.

Unlike the traditional total ion intensity based global normalization method (47), the main algorithm LAXIC introduced here uses for those two factors correction is the local normalization based on library peptide peak intensity ratio in chromatogram. Here we used the plant phosphoproteome as the sample model to assess our method, because plant samples have inherent isotope labeling challenges and the complex metabolome affects the reproducibility of quantitation significantly. This inconsistency of plant phosphopeptide quantification was usually observed during LC-MS based on normalization curve depicted by our internal peptide library. One example, illustrated in Fig. 10, showed a portion of peptides from identical samples with distinguished ratios. We concluded this may be because of the LC-MS condition variation, considering that the normalization curves from these two experiments were differentiated significantly. Interestingly, this deviation was not evenly distributed in the chromatogram, so the global normalization algorithm was not able to compensate such retention time dependent variance. In our experiment, we listed some representative peptides quantitation result from 70 to 80 mins when the environmental conditions varied most (Table II). Those peptides with distinct raw ratios from duplicate experiments were further normalized by either global or local normalization with internal peptide library. As expected, the global normalization, which used the mean ratio of internal standards, did not correct the bias during the 70–80 mins as well as the local normalization process.

The quality performance of LAXIC is highly dependent on a well-designed internal library standard. In particular, hydrophobicity is a simple metric that can describe similarity between peptide library models and proteomic samples. Not only is it desirable for our model system to adhere to the naturally observed hydrophobicity distribution, it is also important to consider potential biases that occur if the distribution for the libraries is out of a practical range. Peptides that are too hydrophobic

might fail to be detected because of insufficient solubility, whereas peptides that are too hydrophilic might not be retained sufficiently on the reverse phase column of the nanoLC system. Because the intrinsic principle of LAXIC quantitation is to locally normalize signal to the internal standards, we propose that high similarity of hydrophobicity between sample and internal standards is desired. supplemental Fig. S7 compares the hydrophobicity distribution of four different libraries (supplemental Table S9), indicating the preference of a particular library toward individual samples.

Although the library peptides are spiked in right before the LC-MS run, the LAXIC method may not be effective to eliminate certain variations introduced by sample preparation in relation to sample clean up, phosphorylation enrichment or other artificial errors during parallel experiments. To further increase the quantitation power of LAXIC, a synthetic phosphopeptide library spiking in the early stage of sample preparation may be applied, resulting in more comprehensive monitoring and error correction.

CONCLUSION

Label-free quantitation by mass spectrometry has emerged as a powerful tool for biological quantifications of complex mixtures. However, a high level of reproducibility is required for the successful application of these methods since the quantification is achieved by inter MS run comparison. Here we introduce a set of spike-in synthetic peptide libraries as internal standards for quality control and reproducibility monitoring of the entire analytical platform for label-free quantitative proteomics experiments. By taking advantage of the statistics within the peptide library, we conducted experiments to demonstrate how LAXIC can effectively monitor sample injection, chromatographic separation, and ion suppression effects to achieve an accurate and robust normalization for the quantitation process. Moreover, needing only regular peptides as the required reagent in LAXIC, this technique is easily conformable to the traditional proteomics platform without requirements of any extra tuning of LC-MS. Great potential exists to expand the local normalization algorithm to other internal standard applications with the merit of a well-designed peptide library that has an even distribution of elution profile throughout the chromatogram. Finally, we demonstrated that LAXIC can be applied to complex quantitative phosphoproteomics experiments to extract biologically valuable results.

Acknowledgments—We thank Katherine Witkin and Jelena Radivojac for help in preparing some of the peptide libraries used in this study.

* This project has been funded in part by an NSF CAREER award CHE-0645020 (W.A.T.), and by National Institutes of Health grants GM088317 (W.A.T.), GM059138 (J.-K.Z.), GM103725 (P.R.), and RR024236 (P.R.).

[S] This article contains supplemental Figs. S1 to S7 and Tables S1 to S9.

‡‡ The corresponding author is the founder and Chief Scientific Officer of Tymora Analytical.

** To whom correspondence should be addressed: Department of Biochemistry, Purdue University, West Lafayette, IN 47907. Tel.: 765-494-9605; Fax: 765-494-7897; E-mail: watao@purdue.edu.

REFERENCES

1. Olsen, J. V., Blagoev, B., Gnad, F., Macek, B., Kumar, C., Mortensen, P., and Mann, M. (2006) Global, in vivo, and site-specific phosphorylation dynamics in signaling networks. *Cell* **127,** 635–648
2. Huttlin, E. L., Jedrychowski, M. P., Elias, J. E., Goswami, T., Rad, R., Beausoleil, S. A., Villén, J., Haas, W., Sowa, M. E., and Gygi, S. P. (2010) A tissue-specific atlas of mouse protein phosphorylation and expression. *Cell* **143,** 1174–1189
3. Zhai, B., Villén, J., Beausoleil, S. A., Mintseris, J., and Gygi, S. P. (2008) Phosphoproteome analysis of Drosophila melanogaster embryos. *J. Proteome Res.* **7,** 1675–1682
4. Ong, S. E., and Mann, M. (2005) Mass spectrometry-based proteomics turns quantitative. *Nat. Chem. Biol.* **1,** 252–262
5. Karisch, R., Fernandez, M., Taylor, P., Virtanen, C., St-Germain, J. R., Jin, L. L., Harris, I. S., Mori, J., Mak, T. W., Senis, Y. A., Östman, A., Moran, M. F., and Neel, B. G. (2011) Global proteomic assessment of the classical protein-tyrosine phosphatome and "Redoxome". *Cell* **146,** 826–840
6. Taus, T., Köcher, T., Pichler, P., Paschke, C., Schmidt, A., Henrich, C., and Mechtler, K. (2011) Universal and confident phosphorylation site localization using phosphoRS. *J. Proteome Res* **10,** 5354–5362
7. Cantin, G. T., Shock, T. R., Park, S. K., Madhani, H. D., and Yates, J. R., 3rd (2007) Optimizing TiO2-based phosphopeptide enrichment for automated multidimensional liquid chromatography coupled to tandem mass spectrometry. *Anal. Chem.* 79, 4666–4673
8. Thingholm, T. E., Jensen, O. N., Robinson, P. J., and Larsen, M. R. (2008) SIMAC (sequential elution from IMAC), a phosphoproteomics strategy for the rapid separation of monophosphorylated from multiply phosphorylated peptides. *Mol. Cell. Proteomics* **7,** 661–671
9. Matsuoka, S., Ballif, B. A., Smogorzewska, A., McDonald, E. R., 3rd, Hurov, K. E., Luo, J., Bakalarski, C. E., Zhao, Z., Solimini, N., Lerenthal, Y., Shiloh, Y., Gygi, S. P., and Elledge, S. J. (2007) ATM and ATR substrate analysis reveals extensive protein networks responsive to DNA damage. *Science* **316,** 1160–1166
10. Trinidad, J. C., Thalhammer, A., Specht, C. G., Lynn, A. J., Baker, P. R., Schoepfer, R., and Burlingame, A. L. (2008) Quantitative analysis of synaptic phosphorylation and protein expression. *Mol. Cell. Proteomics* **7,** 684–696
11. Nguyen, V., Cao, L., Lin, J. T., Hung, N., Ritz, A., Yu, K., Jianu, R., Ulin, S. P., Raphael, B. J., Laidlaw, D. H., Brossay, L., and Salomon, A. R. (2009) A new approach for quantitative phosphoproteomic dissection of signaling pathways applied to T cell receptor activation. *Mol. Cell. Proteomics* **8,** 2418–2431
12. Li, J., Steen, H., and Gygi, S. P. (2003) Protein profiling with cleavable isotope-coded affinity tag (cICAT) reagents: the yeast salinity stress response. *Mol. Cell. Proteomics* **2,** 1198–1204
13. Hoffert, J. D., Pisitkun, T., Wang, G., Shen, R. F., and Knepper, M. A. (2006) Quantitative phosphoproteomics of vasopressin-sensitive renal cells: regulation of aquaporin-2 phosphorylation at two sites. *Proc. Natl. Acad. Sci. U.S.A.* **103,** 7159–7164
14. Stulemeijer, I. J., Joosten, M. H., and Jensen, O. N. (2009) Quantitative phosphoproteomics of tomato mounting a hypersensitive response reveals a swift suppression of photosynthetic activity and a differential role for hsp90 isoforms. *J. Proteome Res.* **8,** 1168–1182
15. Yang, F., Jaitly, N., Jayachandran, H., Luo, Q., Monroe, M. E., Du, X., Gritsenko, M. A., Zhang, R., Anderson, D. J., Purvine, S. O., Adkins, J. N., Moore, R. J., Mottaz, H. M., Ding, S. J., Lipton, M. S., Camp, D. G., 2nd, Udseth, H. R., Smith, R. D., and Rossie, S. (2007) Applying a targeted label-free approach using LC-MS AMT tags to evaluate changes in protein phosphorylation following phosphatase inhibition. *J. Proteome Res.* **6,** 4489–4497
16. Dost, B., Bandeira, N., Li, X., Shen, Z., Briggs, S. P., and Bafna, V. (2012) Accurate mass spectrometry based protein quantification via shared peptides. *J. Comput. Biol.* **19,** 337–348
17. Abshiru, N., Ippersiel, K., Tang, Y., Yuan, H., Marmorstein, R., Verreault, A.,

and Thibault, P. (2012) Chaperone-mediated acetylation of histones by Rtt109 identified by quantitative proteomics. *J. Proteomics* **80,** 80–90
18. Kim, Y. J., Zhan, P., Feild, B., Ruben, S. M., and He, T. (2007) Reproducibility assessment of relative quantitation strategies for LC-MS based proteomics. *Anal. Chem.* **79,** 5651–5658
19. Gerber, S. A., Rush, J., Stemman, O., Kirschner, M. W., and Gygi, S. P. (2003) Absolute quantification of proteins and phosphoproteins from cell lysates by tandem MS. *Proc. Natl. Acad. Sci. U.S.A.* **100,** 6940–6945
20. Monetti, M., Nagaraj, N., Sharma, K., and Mann, M. (2011) Large-scale phosphosite quantification in tissues by a spike-in SILAC method. *Nat. Methods* **8,** 655–658
21. Tabata, T., Sato, T., Kuromitsu, J., and Oda, Y. (2007) Pseudo internal standard approach for label-free quantitative proteomics. *Anal. Chem.* **79,** 8440–8445
22. Liu, X., Miller, B. R., Rebec, G. V., and Clemmer, D. E. (2007) Protein expression in the striatum and cortex regions of the brain for a mouse model of Huntington's disease. *J. Proteome Res.* **6,** 3134–3142
23. Sherrod, S. D., Myers, M. V., Li, M., Myers, J. S., Carpenter, K. L., Maclean, B., Maccoss, M. J., Liebler, D. C., and Ham, A. J. (2012) Label-Free Quantitation of Protein Modifications by Pseudo Selected Reaction Monitoring with Internal Reference Peptides. *J. Proteome Res.* **11(6),** 3467–3479
24. Han, C. L., Chen, J. S., Chan, E. C., Wu, C. P., Yu, K. H., Chen, K. T., Tsou, C. C., Tsai, C. F., Chien, C. W., Kuo, Y. B., Lin, P. Y., Yu, J. S., Hsueh, C., Chen, M. C., Chan, C. C., Chang, Y. S., and Chen, Y. J. (2011) An informatics-assisted label-free approach for personalized tissue membrane proteomics: case study on colorectal cancer. *Mol. Cell. Proteomics* 10, M110.003087
25. Bondarenko, P. V., Chelius, D., and Shaler, T. A. (2002) Identification and relative quantitation of protein mixtures by enzymatic digestion followed by capillary reversed-phase liquid chromatography-tandem mass spectrometry. *Anal. Chem.* **74,** 4741–4749
26. Wang, W., Zhou, H., Lin, H., Roy, S., Shaler, T. A., Hill, L. R., Norton, S., Kumar, P., Anderle, M., and Becker, C. H. (2003) Quantification of proteins and metabolites by mass spectrometry without isotopic labeling or spiked standards. *Anal Chem.* **75,** 4818–4826
27. Zhang R, B. A., Brittenden J, Huang JT, Crowther D (2010) Evaluation for computational platforms of LC-MS based label-free quantitative proteomics: A global view. *J. Proteomics Bioinformatics* **3,** 260–265
28. Xie, F., Liu, T., Qian, W. J., Petyuk, V. A., and Smith, R. D. (2011) Liquid chromatography-mass spectrometry-based quantitative proteomics. *J. Biol. Chem.* **286,** 25443–25449
29. Zybailov, B., Mosley, A. L., Sardiu, M. E., Coleman, M. K., Florens, L., and Washburn, M. P. (2006) Statistical analysis of membrane proteome expression changes in Saccharomyces cerevisiae. *J. Proteome Res.* **5,** 2339–2347
30. Reiland, S., Messerli, G., Baerenfaller, K., Gerrits, B., Endler, A., Grossmann, J., Gruissem, W., and Baginsky, S. (2009) Large-scale Arabidopsis phosphoproteome profiling reveals novel chloroplast kinase substrates and phosphorylation networks. *Plant Physiol.* **150,** 889–903
31. Cox, J., and Mann, M. (2008) MaxQuant enables high peptide identification rates, individualized p.p.b.-range mass accuracies and proteome-wide protein quantification. *Nat. Biotechnol* **26,** 1367–1372
32. Jaffe, J. D., Mani, D. R., Leptos, K. C., Church, G. M., Gillette, M. A., and Carr, S. A. (2006) PEPPeR, a platform for experimental proteomic pattern recognition. *Mol. Cell. Proteomics* **5,** 1927–1941
33. MacLean, B., Tomazela, D. M., Shulman, N., Chambers, M., Finney, G. L., Frewen, B., Kern, R., Tabb, D. L., Liebler, D. C., and MacCoss, M. J. (2010) Skyline: an open source document editor for creating and analyzing targeted proteomics experiments. *Bioinformatics* **26,** 966–968
34. Bolstad, B. M., Irizarry, R. A., Astrand, M., and Speed, T. P. (2003) A comparison of normalization methods for high density oligonucleotide array data based on variance and bias. *Bioinformatics* **19,** 185–193
35. Urao, T., Yakubov, B., Satoh, R., Yamaguchi-Shinozaki, K., Seki, M., Hirayama, T., and Shinozaki, K. (1999) A Transmembrane Hybrid-Type Histidine Kinase in Arabidopsis Functions as an Osmosensor. *Plant Cell Online* **11,** 1743–1754
36. Wohlbach, D. J., Quirino, B. F., and Sussman, M. R. (2008) Analysis of the Arabidopsis Histidine Kinase ATHK1 Reveals a Connection between Vegetative Osmotic Stress Sensing and Seed Maturation. *Plant Cell Online* **20,** 1101–1117
37. Mikołajczyk, M., Awotunde, O. S., Muszyńska, G., Klessig, D. F., and Dobrowolska, G. (2000) Osmotic Stress Induces Rapid Activation of a Salicylic Acid,ÄìInduced Protein Kinase and a Homolog of Protein Kinase ASK1 in Tobacco Cells. *Plant Cell Online* **12,** 165–178
38. Ichimura, K., Mizoguchi, T., Yoshida, R., Yuasa, T., and Shinozaki, K. (2000) Various abiotic stresses rapidly activate Arabidopsis MAP kinases ATMPK4 and ATMPK6. *Plant J.* **24,** 655–665
39. Kim, J. M., Woo, D. H., Kim, S. H., Lee, S. Y., Park, H. Y., Seok, H. Y., Chung, W., and Moon, Y. H. (2012) Arabidopsis MKKK20 is involved in osmotic stress response via regulation of MPK6 activity. *Plant Cell Reports* **31,** 217–224
40. Franz, S., Ehlert, B., Liese, A., Kurth, J., Cazalé, A.-C., and Romeis, T. (2011) Calcium-Dependent Protein Kinase CPK21 Functions in Abiotic Stress Response in Arabidopsis thaliana. *Molecular Plant* **4,** 83–96
41. Xu, J., Tian, Y. S., Peng, R. H., Xiong, A. S., Zhu, B., Jin, X. F., Gao, F., Fu, X. Y., Hou, X. L., and Yao, Q. H. (2010) AtCPK6, a functionally redundant and positive regulator involved in salt/drought stress tolerance in Arabidopsis. *Planta* **231,** 1251–1260
42. Saijo, Y., Hata, S., Kyozuka, J., Shimamoto, K., and Izui, K. (2000) Over-expression of a single Ca2+-dependent protein kinase confers both cold and salt/drought tolerance on rice plants. *Plant J.* **23,** 319–327
43. Boudsocq, M., Barbier-Brygoo, H., and Laurière, C. (2004) Identification of Nine Sucrose Nonfermenting 1-related Protein Kinases 2 Activated by Hyperosmotic and Saline Stresses in Arabidopsis thaliana. *J. Biol. Chem.* **279,** 41758–41766
44. Fujii, H., and Zhu, J.-K. (2009) Arabidopsis mutant deficient in 3 abscisic acid-activated protein kinases reveals critical roles in growth, reproduction, and stress. *Proc. Natl. Acad. Sci. U. S. A.***106,** 8380–8385
45. Fujii, H., Verslues, P. E., and Zhu, J. K. (2011) Arabidopsis decuple mutant reveals the importance of SnRK2 kinases in osmotic stress responses in vivo. *Proc. Natl. Acad. Sci. U.S.A.* **108,** 1717–1722
46. Fujii, H., and Zhu, J. K. (2012) Osmotic stress signaling via protein kinases. *Cell Mol. Life Sci.* **69(19),** 3165–3173
47. Casado, P., and Cutillas, P. R. (2011) A self-validating quantitative mass spectrometry method for assessing the accuracy of high-content phosphoproteomic experiments. *Mol. Cell. Proteomics* 10, M110.003079
48. Bohrer, B. C., Li, Y. F., Reilly, J. P., Clemmer, D. E., DiMarchi, R. D., Radivojac, P., Tang, H., and Arnold, R. J. (2010) Combinatorial Libraries of Synthetic Peptides as a Model for Shotgun Proteomics. *Anal. Chem.* **82,** 6559–6568
49. Lebl, M., and Krchnak, V. (1997) Synthetic peptide libraries. *Method Enzymol.* **289,** 336–392
50. Iliuk, A. B., Martin, V. A., Alicie, B. M., Geahlen, R. L., and Tao, W. A. (2010) In-depth analyses of kinase-dependent tyrosine phosphoproteomes based on metal ion-functionalized soluble nanopolymers. *Mol. Cell. Proteomics* **9,** 2162–2172
51. Bertsch, A., Gropl, C., Reinert, K., and Kohlbacher, O. (2011) OpenMS and TOPP: Open Source Software for LC-MS Data Analysis. *Data Mining in Proteomics: From Standards to Applications* **696,** 353–367
52. Oeljeklaus, S., Meyer, H. E., and Warscheid, B. (2009) Advancements in plant proteomics using quantitative mass spectrometry. *J. Proteomics* **72,** 545–554
53. Kline, K. G., Barrett-Wilt, G. A., and Sussman, M. R. (2010) In planta changes in protein phosphorylation induced by the plant hormone abscisic acid. *Proc. Natl. Acad. Sci. U.S.A.* **107,** 15986–15991
54. Deleted in proof
55. Alcolea, M. P., Kleiner, O., and Cutillas, P. R. (2009) Increased confidence in large-scale phosphoproteomics data by complementary mass spectrometric techniques and matching of phosphopeptide data sets. *J. Proteome Res.* **8,** 3808–3815
56. Villén, J., Beausoleil, S. A., Gerber, S. A., and Gygi, S. P. (2007) Large-scale phosphorylation analysis of mouse liver. *Proc. Natl. Acad. Sci. U.S.A.* **104,** 1488–1493
57. Wu, R., Dephoure, N., Haas, W., Huttlin, E. L., Zhai, B., Sowa, M. E., and Gygi, S. P. (2011) Correct interpretation of comprehensive phosphorylation dynamics requires normalization by protein expression changes. *Mol. Cell. Proteomics* 10, M111.009654
58. Sassi, S., Aydi, S., Hessini, K., Gonzalez, E. M., Arrese-Igor, C., and Abdelly, C. (2010) Long-term mannitol-induced osmotic stress leads to stomatal closure, carbohydrate accumulation and changes in leaf elasticity in Phaselous vulgaris leaves. *Afr. J. Biotechnol.* **9,** 6061–6069

59. Szklarczyk, D., Franceschini, A., Kuhn, M., Simonovic, M., Roth, A., Minguez, P., Doerks, T., Stark, M., Muller, J., Bork, P., Jensen, L. J., and von Mering, C. (2011) The STRING database in 2011: functional interaction networks of proteins, globally integrated and scored. *Nucleic Acids Res.* **39,** D561–D568
60. Schwartz, D., and Gygi, S. P. (2005) An iterative statistical approach to the identification of protein phosphorylation motifs from large-scale data sets. *Nat. Biotechnol.* **23,** 1391–1398
61. Riera, M., Figueras, M., López, C., Goday, A., and Pagès, M. (2004) Protein kinase CK2 modulates developmental functions of the abscisic acid responsive protein Rab17 from maize. *Proc. Natl. Acad. Sci. U.S.A.* **101,** 9879–9884
62. Fujita, Y., Fujita, M., Shinozaki, K., and Yamaguchi-Shinozaki, K. (2011) ABA-mediated transcriptional regulation in response to osmotic stress in plants. *J. Plant Res.* **124,** 509–525
63. Vlad, F., Turk, B. E., Peynot, P., Leung, J., and Merlot, S. (2008) A versatile strategy to define the phosphorylation preferences of plant protein kinases and screen for putative substrates. *Plant J.* **55,** 104–117
64. Qi, X., Wu, Z., Li, J., Mo, X., Wu, S., Chu, J., and Wu, P. (2007) AtCYT-INV1, a neutral invertase, is involved in osmotic stress-induced inhibition on lateral root growth in Arabidopsis. *Plant Mol. Biol.* **64,** 575–587
65. de Silva, K., Laska, B., Brown, C., Sederoff, H. W., and Khodakovskaya, M. (2011) Arabidopsis thaliana calcium-dependent lipid-binding protein (AtCLB): a novel repressor of abiotic stress response. *J. Exp. Botany* **62,** 2679–2689
66. dit Frey, N. F., Muller, P., Jammes, F., Kizis, D., Leung, J., Perrot-Rechenmann, C., and Bianchi, M. W. (2010) The RNA Binding Protein Tudor-SN Is Essential for Stress Tolerance and Stabilizes Levels of Stress-Responsive mRNAs Encoding Secreted Proteins in Arabidopsis. *Plant Cell Online* **22,** 1575–1591
67. Humphry, M., Bednarek, P., Kemmerling, B., Koh, S., Stein, M., Gobel, U., Stuber, K., Pislewska-Bednarek, M., Loraine, A., Schulze-Lefert, P., Somerville, S., and Panstruga, R. (2010) A regulon conserved in monocot and dicot plants defines a functional module in antifungal plant immunity. *Proc. Natl. Acad. Sci. U. S. A.* **107,** 21896–21901
68. Christensen, A., Svensson, K., Persson, S., Jung, J., Michalak, M., Widell, S., and Sommarin, M. (2008) Functional Characterization of Arabidopsis Calreticulin1a: A Key Alleviator of Endoplasmic Reticulum Stress. *Plant Cell Physiol.* **49,** 912–924
69. Qiu, Y., Xi, J., Du, L., Roje, S., and Poovaiah, B. W. (2012) A dual regulatory role of Arabidopsis calreticulin-2 in plant innate immunity. *Plant J.* **69,** 489–500
70. Trotta, A., Wrzaczek, M., Scharte, J., Tikkanen, M., Konert, G., Rahikainen, M., Holmström, M., Hiltunen, H. M., Rips, S., Sipari, N., Mulo, P., Weis, E., von Schaewen, A., Aro, E. M., and Kangasjarvi, S. (2011) Regulatory subunit B'gamma of protein phosphatase 2A prevents unnecessary defense reactions under low light in Arabidopsis. *Plant Physiol.* **156,** 1464–1480